

Supplementary Materials and Methods

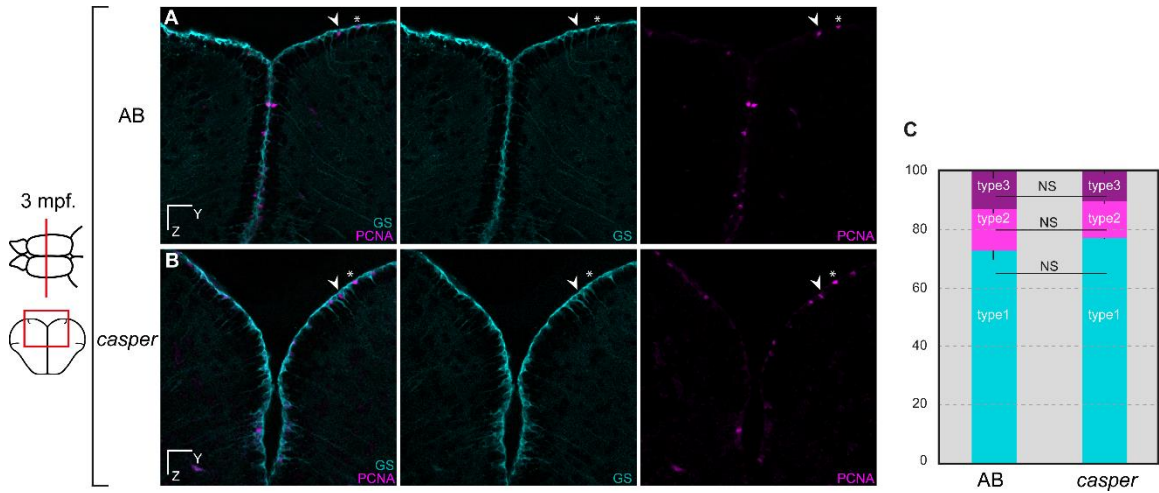
Generation of the *Tg(mcm5:egfp)^{gy2}* transgenic line. A 1,200 bp *mcm5* enhancer region was amplified by PCR using zebrafish wildtype (AB line) genomic DNA as template. The genomic DNA was used in a standard 50µL volume PCR using *Taq* DNA polymerase (EmeraldAmp Takara, Cat# 330A) with forward primer 5'-TTCATTACACCAGGGGTTCA) and reverse primer (5'-GCCTCAGAAACTCACGGAAC). A second PCR was done using 1µL of the PCR product from the first PCR and forward primer (5'-GGGGCAACTTTGTATAGAAAAGTTGTTTCATTACACCAGGGGTTTCA) and reverse primer (5'-GGGGCTGCTTTTTTTGTACAACTTGTCCTCGACATTCTTGCAAA). The PCR cycle parameters were (i) hotstart 94°C for 2 min; (ii) denaturation, 94°C for 10s; (iii) annealing, 59°C for 30s for PCR1 and 55°C for 30 s for PCR2; (iv) elongation, 72°C for 1m30s; repeated for 35 cycles. The PCR product was purified using the Nucleospin ExtractII kit (Macherey Nagel, Cat#740609) and subcloned into the destination vector pDestTol2pA2 using the gateway technology v1.2. The transgenic line *Tg(mcm5:eGFP)* was made by co-injecting 1-cell embryos with a mix containing 13.75ng/µL of this plasmid and 15ng/µL of transposase capped RNA. F0 adults were screened for transmission by crossing into wildtype fish and recording fluorescence in F1 embryos.

Fish anesthesia and mounting for imaging. Several protocols for long-term anesthesia were compared (supplementary material Table 1) and protocol 3 was selected for further experiments based on its efficiency to immobilize animals and its high associated survival rate. To reduce respiratory movements during the imaging acquisition, the opercula covering the gills were gently removed at least a couple of days before the first day of imaging. Anesthesia was induced with 0.02% MS222 (Tricaine) for approximately 90 seconds until immobilization was observed, and anesthetized fish were mounted in a home-made plastic dish between pieces of sponge. To maintain anesthesia, the fish were intubated with a small truncated tip letting flow a 0.005% Tricaine, 0.005% Isoflurane solution. The same solution was used to fill up the plastic dish. We used a flow of about 100mL per hour. The excess of liquid was pumped out using a peristaltic pump. From the second imaging time point onwards, we used the harmonic signals to approximately orient the fish in a position similar to previous time points.

Image cross-correlation analyses

3D image cross-correlation was computed using Matlab based on the “normxcorr3” Matlab function provided by Daniel Eaton (<http://www.cs.ubc.ca/deaton/tut/normxcorr3.html>). This

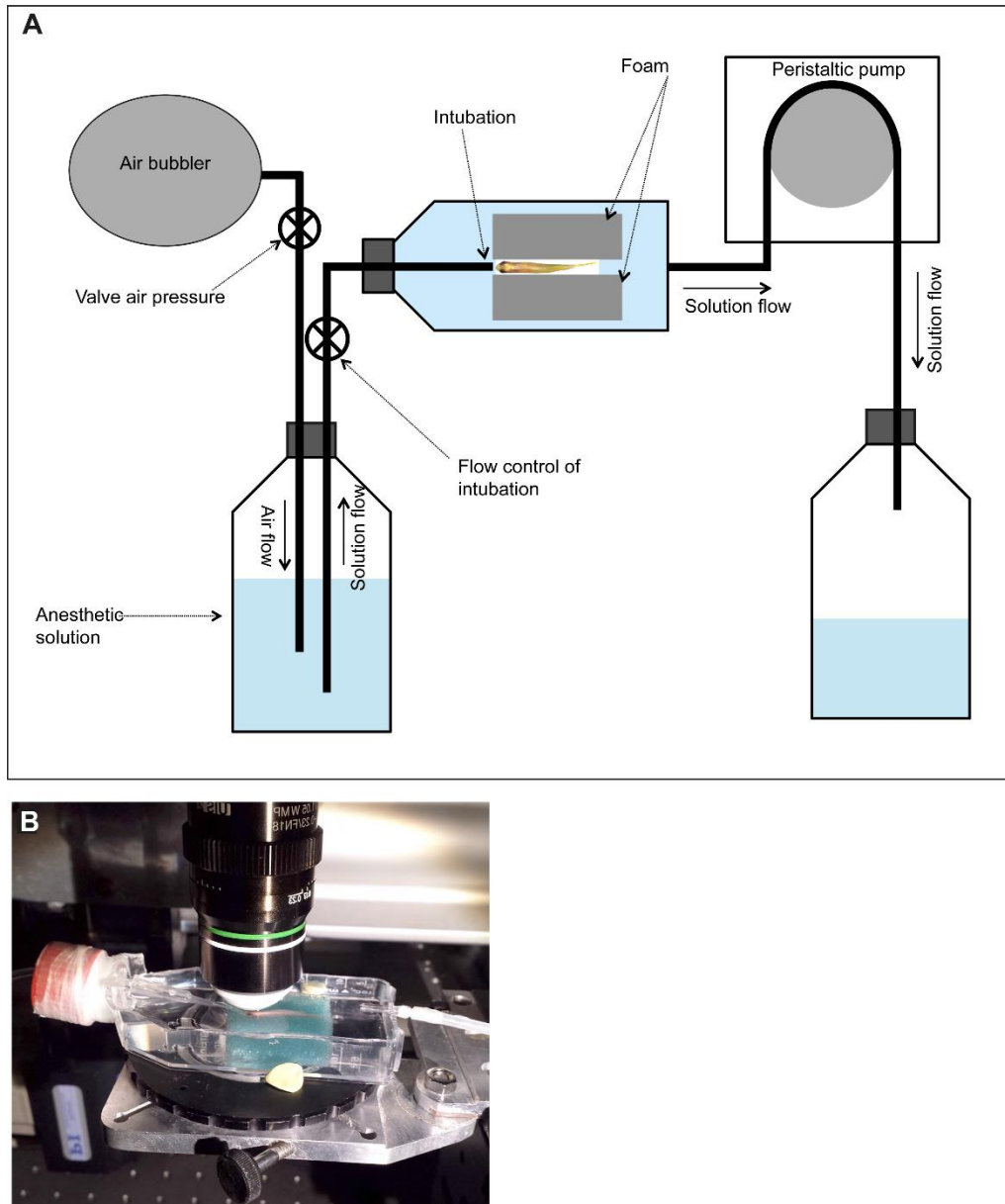
fast 3D normalized cross correlation tool is the 3D extension of “normxcorr2” Matlab function. Cross-correlation was performed between two successive time points and using 40x40x40 μm^3 (or 48x38x20 voxels) cubic interrogation volumes centered around the segmented position of cells. Cross-correlation volumes were estimated for 100 of tracked cells (11 only in the fish named *fifi*). Within these correlation volumes, the correlation peak amplitude provides an estimation of how well the pattern of signal surrounding a cell matches from one time point to the next (1 for a perfect match and 0 for no correlation). In addition, in the case of a significant correlation amplitude, the relative position of this peak to the center of the correlation volume estimates the local displacement of the pattern from one time point to the next: it estimates the error of image alignment at the scale of the few cells contained within the interrogation volume. In all our experiments, this displacement was below the cell size (typically $< 5\mu\text{m}$), which corresponds to the error of cell position estimation. The correlation values plotted in Fig 6B and 6D correspond to the peak amplitude when the peak location is close to the center ($<10\mu\text{m}$ away) or the correlation at the center of the correlation volume otherwise (when the correlation is poor and the correlation peak position is meaningless). In these figures, the control measurement was performed by running the same analysis after random permutation of cell positions. In all cases, the average correlation value of tracked cells is significantly higher than the control (Welch’s test with $p\text{-value} < 2.10^{-7}$).



Supplementary material Fig. S1. Adult *casper* fish¹ display a normal profile of telencephalic neural progenitors.

(A,B) Cross-sections of the telencephalon and immunostaining for the glial marker GS (cyan) and the proliferation marker PCNA (magenta) in the pallium of 3 month-old (mpf) (A) wild type AB and (B) *casper* (double homozygote for *roy*^{-/-}; *nacre*^{-/-}) zebrafish. (C) Quantification of non-dividing RG (type1 cells), dividing RG (type2 cells) (arrowhead) and dividing non-RG (type3 cells) (asterisk) progenitors showing no statistical differences between the two genotypes (unpaired t-test comparing the proportion of each cell type between AB and *casper*, *P* values > 0.05) (unpaired t-test for type1 cells: *P* value = 0.0821; for type 2 cells: *P* value = 0.1477; for type 3 cells: *P* value = 0.0974). n = 4 brains each with 3 to 6 sections per brain.

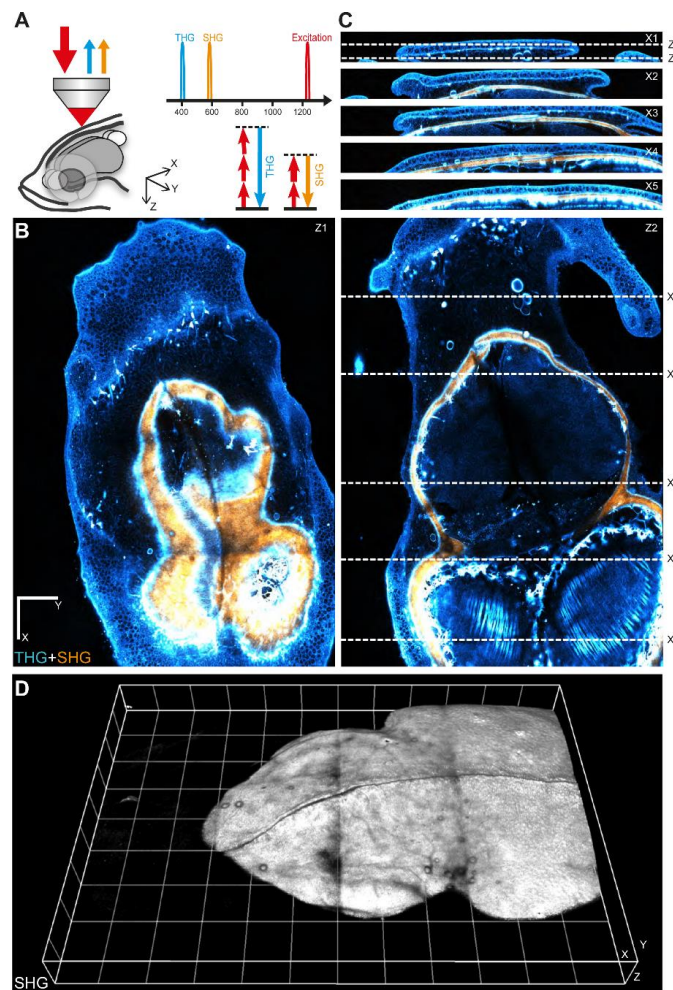
Scale bars: 30 μ m (A,B)



Supplementary material Fig. S2. Anesthesia procedure and fish holding set up.

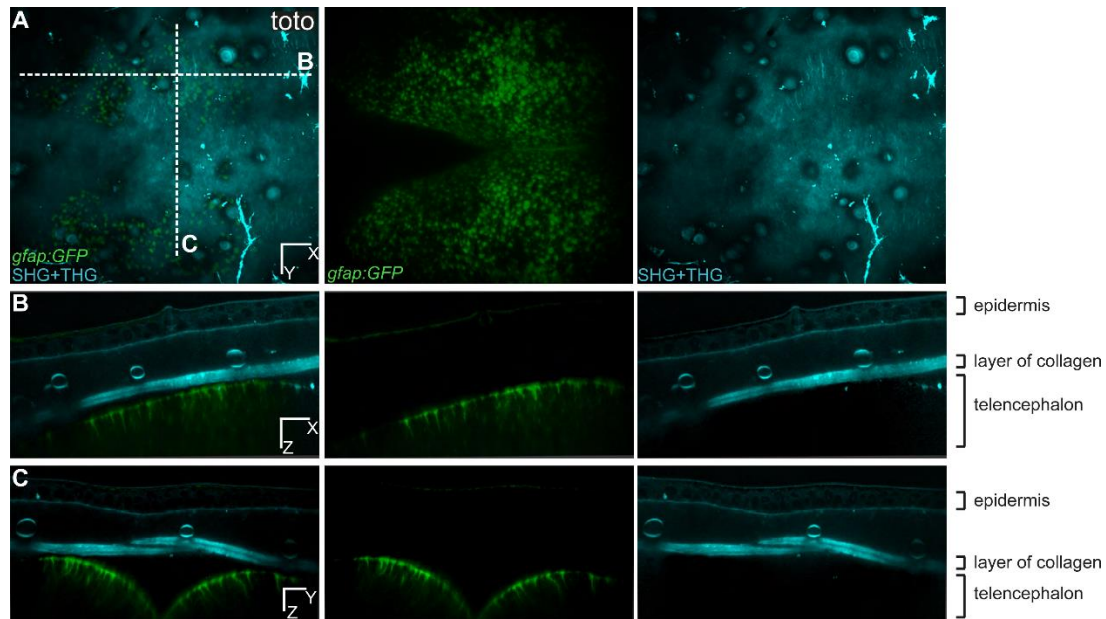
(A) Set up to mount the adult zebrafish. After anesthesia for 1min in 0.02% Tricaine the fish is mounted and maintained in a plastic dish between pieces of sponge. To maintain the anesthesia the fish is intubated with a small truncated tip letting flow a 0.005% Tricaine, 0.005% Isoflurane solution. The same solution is used to fill up the plastic dish. We used a flow of about 100mL per hour. The excess of liquid is pumped out using a peristaltic pump.

(B) Picture of the plastic dish holding a 3 month-old *casper* zebrafish.



Supplementary material Fig. S3. Second- and third-harmonic generation (SHG, THG) imaging of the telencephalon region in a live zebrafish adult.

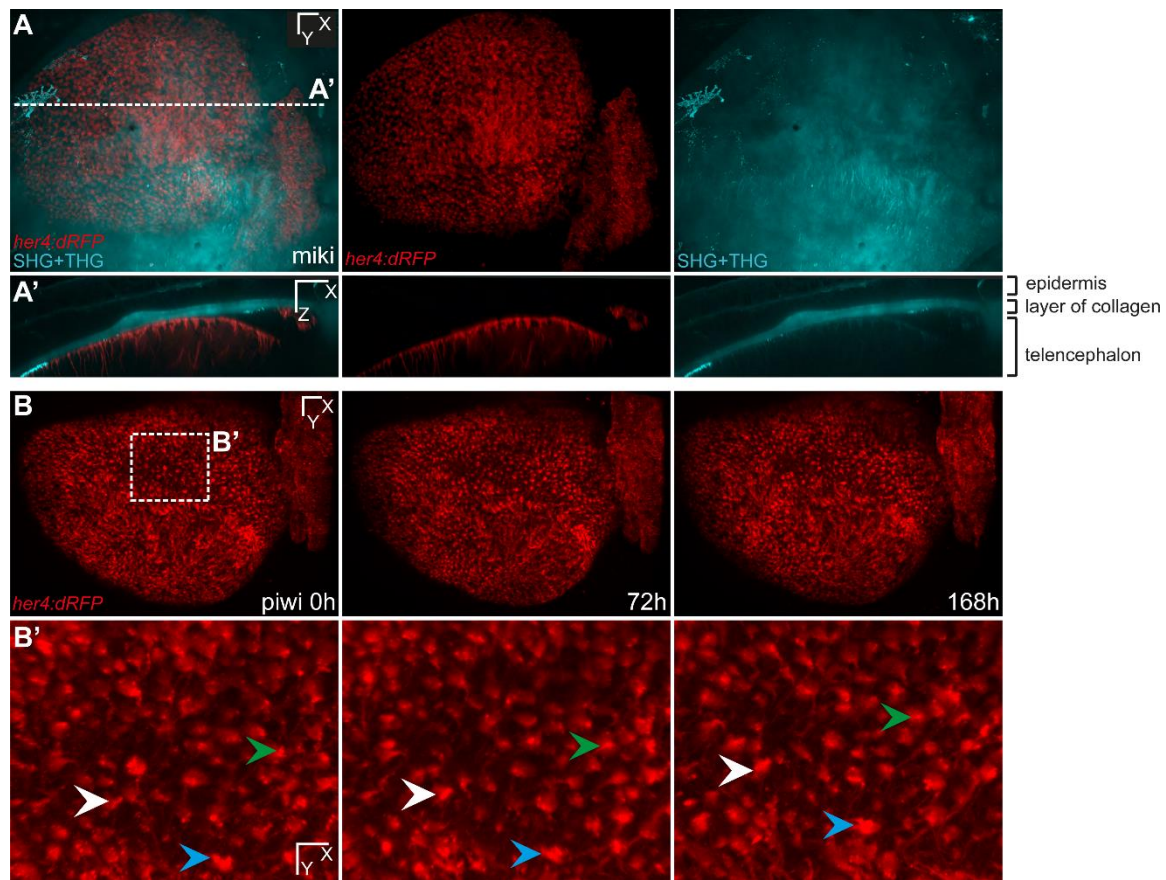
(A) Imaging geometry and harmonic signals optical properties. The fish (5 months) was anesthetized and held in an upright microscope. Backscattered THG and SHG signals were collected through the excitation objective. X corresponds the antero-posterior (ap) axis, Y corresponds to the left-right (lr) axis, and Z corresponds to the dorso-ventral (dv) axis. (B) Two XY images extracted from a dataset encompassing a $2380 \times 1708 \times 160 \mu\text{m}^3$ volume. (C) Four YZ images extracted from the same dataset. The entire dataset consists of a mosaic of 12 XYZ stacks acquired with $500 \mu\text{m}$ lateral steps, each spanning a volume of $800 \times 800 \times 180 \mu\text{m}^3$. The global image was assembled from the raw XYZ stacks using FIJI grid stitching module. Excitation wavelength was $\lambda = 1180 \text{ nm}$. THG signals (at $\lambda/3$) and SHG signals (at $\lambda/2$) were simultaneously detected on two independent channels. The SHG image, shown in orange, highlights fibrillar collagen and reveals the global structure of the skull. The THG image, shown in blue, highlights interfaces and heterogeneities and provides multiple structural details. In particular, THG signals reveal skin cell boundaries, blood vessels, pigmented cells, skull surface, lipidic accumulations, and myelin fibers. Scale bar, $200 \mu\text{m}$. Voxel size $2 \times 2 \times 2 \mu\text{m}^3$. Time per pixel $5 \mu\text{s}$. (D) 3D rendering of the SHG data, revealing skull structure. Grid size, $200 \mu\text{m}$. 3D rendering was calculated using Imaris (Bitplane). See also Supplementary material Movies 1, 2 and 3.



Supplementary material Fig. S4. Multicolor 3D images of RG cells in the pallium and SHG/THG signals of the structures above.

Dorsal (A), transversal (B) and cross (C) views for one time point of a transgenic zebrafish *gfap:eGFP* into a *casper* background (individual fish named toto). The green channel is showing all the glial cells and the processes are visible (B, C). The cyan channel is showing structures such as collagen, lipids, light-absorbing cells, and the epidermis, where individual cells are visible. The merged panel in (C) is the same as on Fig.1C.

Scale bars, 50 μ m (A,-C).

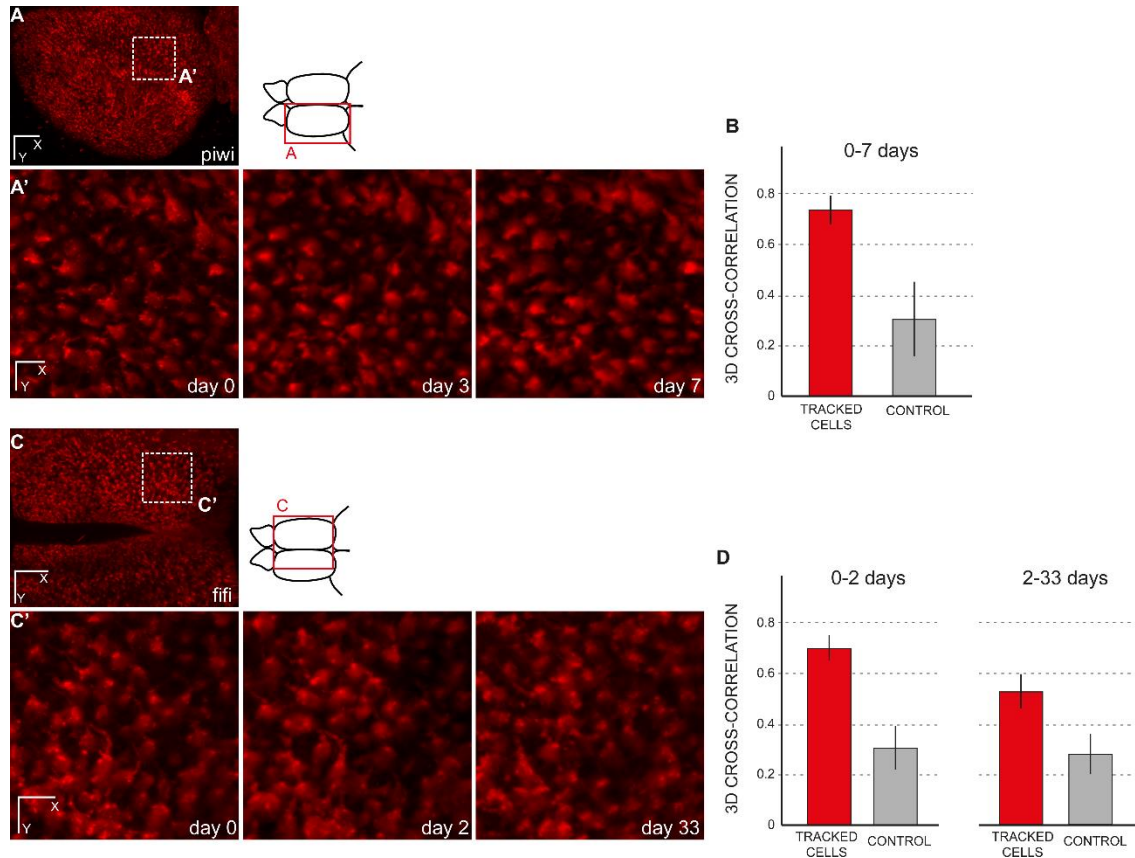


Supplementary material Fig. 5. Alignment of successive z-stacks using SHG/THG signals.

(A,A') Dorsal and transversal views respectively for one time point of a transgenic zebrafish *her4:dRFP* into a *casper* background (individual fish named miki). The red channel is showing all the glial cells expressing Her4 and their processes are visible (A'). One entire hemisphere can be imaged using the 20X objective such as in (A) or two halves of each hemisphere such as in Supplementary material Fig. S3.

(B,B') Three time points of a transgenic *her4:dRFP* named piwi. The time points were aligned using the SHG/THG signals only (not shown here) and the RecursiveReg Imaris extension. (B') is showing a high magnification of (B) and the three arrowheads are pointing to the same three cells over 168 hours showing that the alignment almost perfectly corrects the changes in orientation when the fish is repeatedly mounted (see also Supplementary material Movie 4).

Scale bars, 50 μ m (A-B), 20 μ m (B').

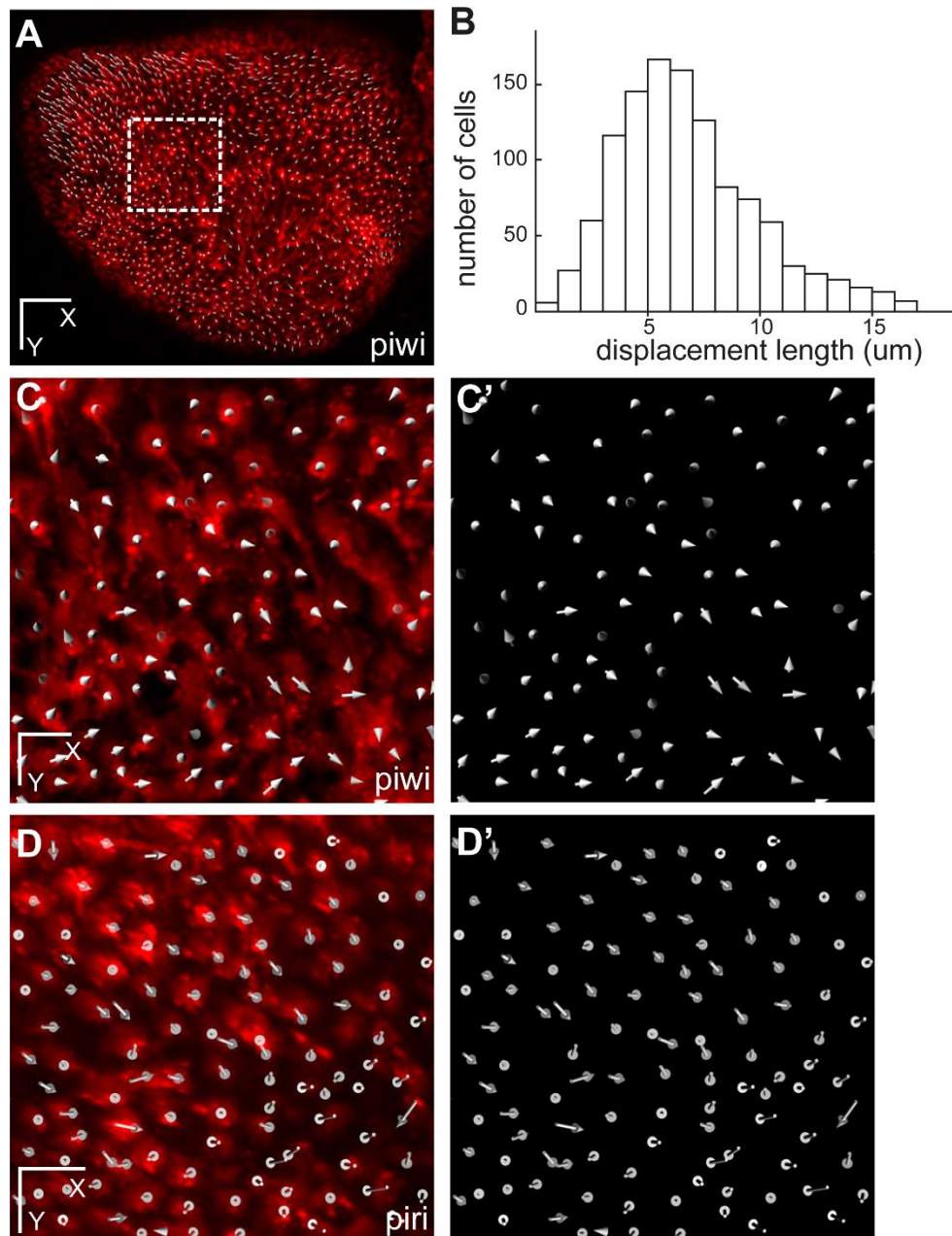


Supplementary material Fig. S6. Cross-correlation of randomly chosen cells between time points.

(A,A') Dorsal general view and close up for three time points (until 7 days) of a transgenic zebrafish *her4:drFP* into a *casper* background (individual fish named piwi). (A') shows the result for the area boxed in A after a manual re-alignment using the drift correction in the Imaris software (Bitplane). (B) Amplitude of 3D image cross-cross correlations of 100 tracked cells between day 0 and day 3 or between day 3 and day 7. The average correlation of tracked cells is significantly higher than the control case, when the same analysis is performed after random permutation of cell positions (Welch's test, $p=1.2 \cdot 10^{-118}$).

(C,C') Dorsal general view and close up for three time points (until 33 days) of a transgenic zebrafish *her4:drFP* into a *casper* background (individual fish named fifi). (C') shows the result for the area boxed in A after a manual re-alignment using the drift correction in the Imaris software (Bitplane). (D) Amplitude of 3D image cross-cross correlations of 11 tracked cells between day 0 and day 2 (left) and between day 2 and day 33 (right). As expected, the correlation amplitude decreases for longer delay between time points (here, from 0.70 for 2 days, to 0.53 for 31 days). However, in both cases the average correlation of tracked cells remains significantly higher than the control case, when the same analysis is performed after random permutation of cell positions (Welch's test, $p=5.1 \cdot 10^{-10}$ and $p=1.7 \cdot 10^{-7}$, respectively).

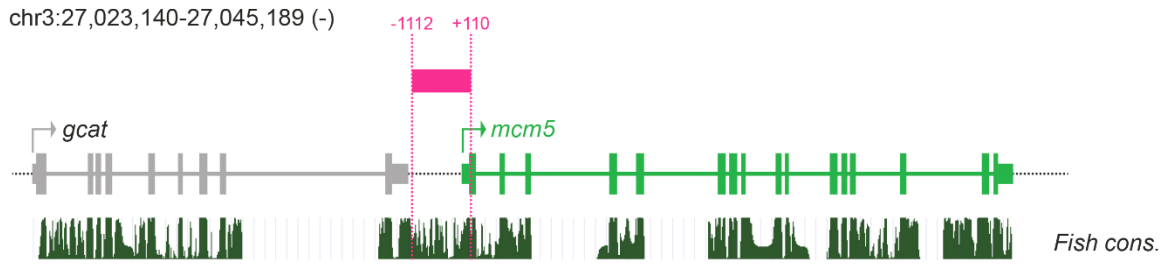
Scale bars: 80 μm (A, C), 20 μm (A', C'),



Supplementary material Fig. S7. Absence of migration of pallial RG cells.

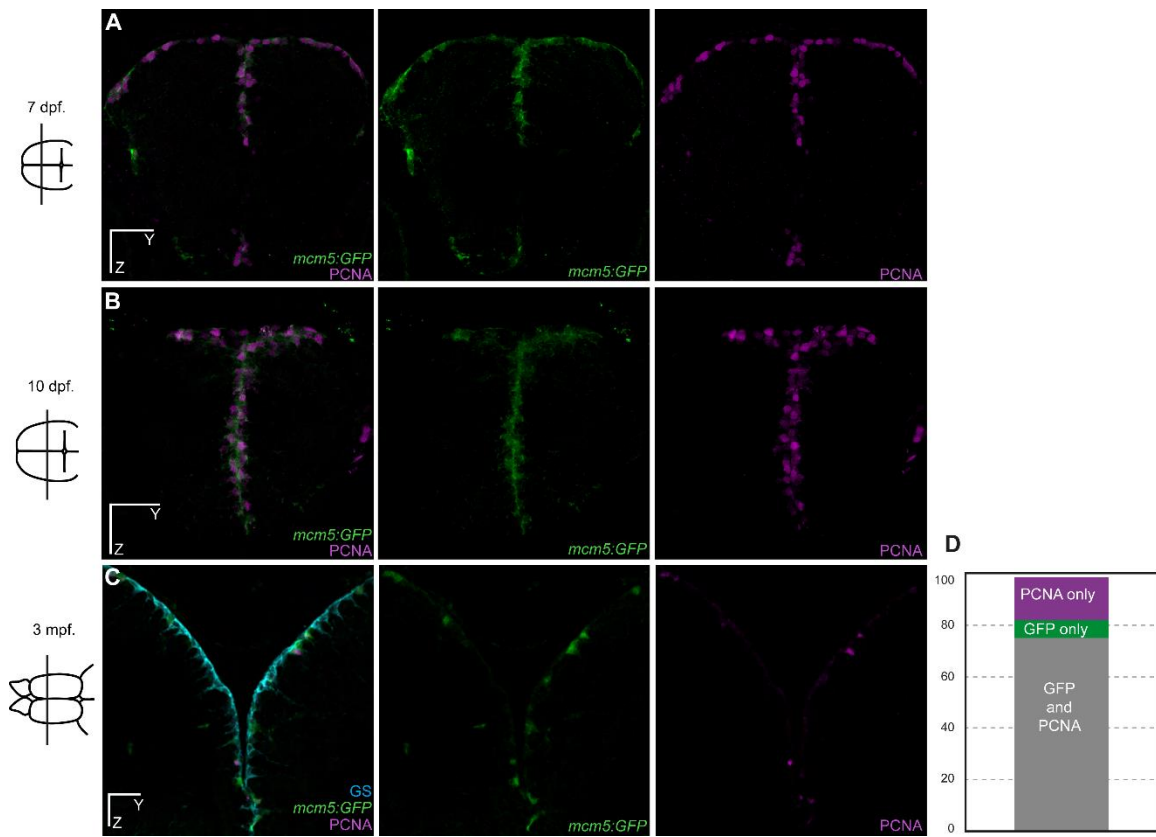
(A) Dorsal view of the entire pallial germinal zone of one telencephalic hemisphere in a transgenic zebrafish *her4:drFP* into a *casper* background (individual fish named piwi) at $t=0$, where all individual RG cells have been plotted (white dots, 1,122 cells). (B) Distribution of the total displacement length of each of the 1,122 cells after 7 days of imaging. The gaussian curve, with an average displacement of $6.59 \mu\text{m}$ ($\text{SD}=2.4$) does not reveal outlier cells (Grubbs' test). (C,C') Overall displacement vector of each individual cell after 7 days of imaging in the area boxed in A (C: vectors shown on top of red fluorescence -RG cells-, C': vectors only). Note in C that the average displacement of each cell rarely exceed the size of a cell diameter. (D,D') Same representations as (C,C') but for an equivalent area in the individual fish named piri. Of note, in the case of a division, daughter cells, which always remain adjacent (see Fig. 2), have been plotted as a single cell.

Scale bars: $80 \mu\text{m}$ (A), $20 \mu\text{m}$ (C-D').



Supplementary material Fig. S8. 1.2 kb upstream region of *mcm5* genomic DNA used to generate *Tg(mcm5:eGFP)^{gy2}*.

The amplified fragment, located on chromosome 3 at the position indicated, also contains the *mcm5* 5' UTR and ATG (located in position +110 relative to the transcription start site, indicated by the green arrow). Stretches of sequence conservation with other fish genomes (Tetraodon, Medaka, Stickleback, Fugu) is indicated below the schematized *mcm5* genomic locus.



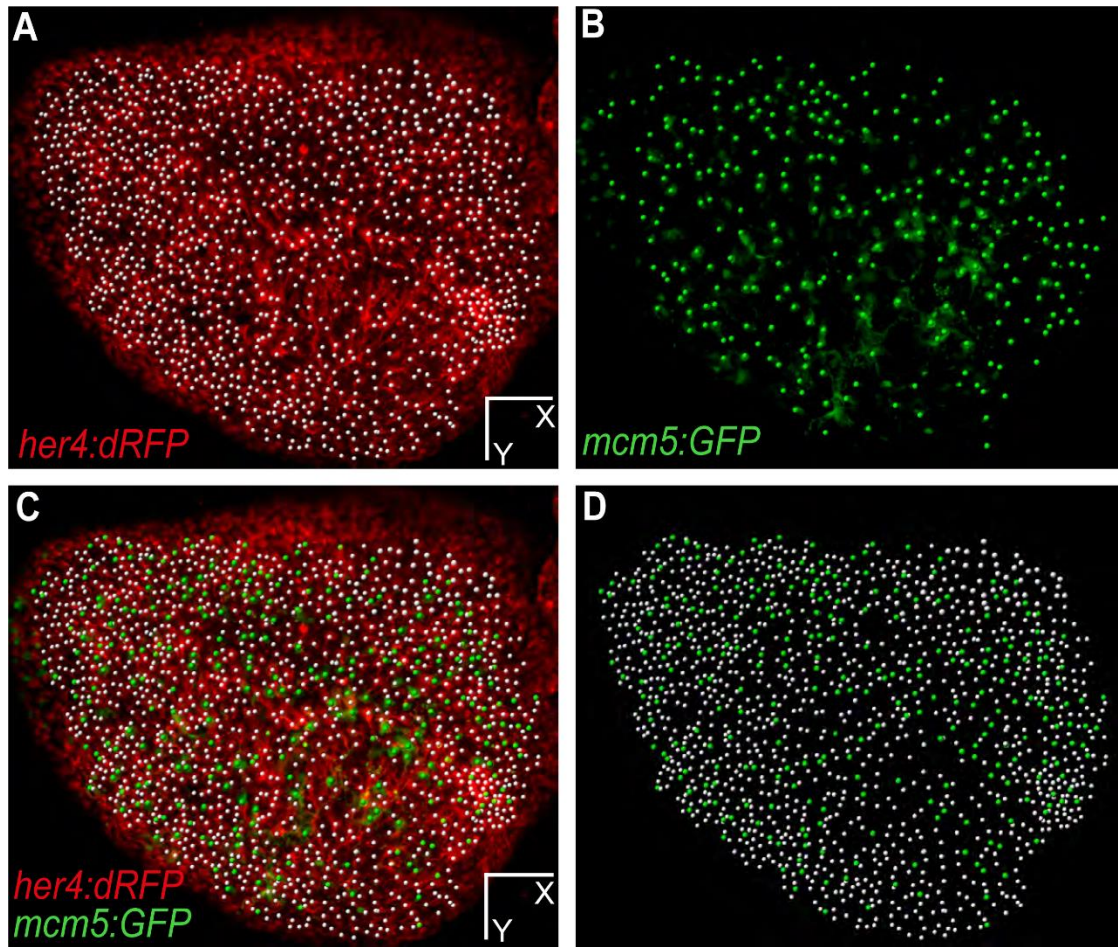
Supplementary material Fig. S9. Validation of the *Tg(mcm5:eGFP)^{gy2}* transgenic line for the reliable reporting of neural progenitor cell division in the zebrafish pallium.

(A-C) Cross-sections of the telencephalon are shown in transgenic zebrafish at 7 day-post-fertilization (dpf), 10 dpf and 3 month-post-fertilization (mpf) with double immunostaining for the proliferation marker PCNA (magenta) and GFP (green).

(D) Quantification showing that GFP is strictly co-expressed with PCNA in 75% (sem=3.1) of the positive ventricular progenitors (sum of PCNA and MCM5 cells). 17% (sem=4.0) of the positive cells express GFP only, which we interpret as cells having divided but still maintaining some GFP protein due to GFP stability. 8% (sem=1.8) of the positive cells express PCNA only, which we interpret as cell just entering the cell cycle with no GFP detectable yet.

n = 4 brains each with 3 to 6 sections per brain.

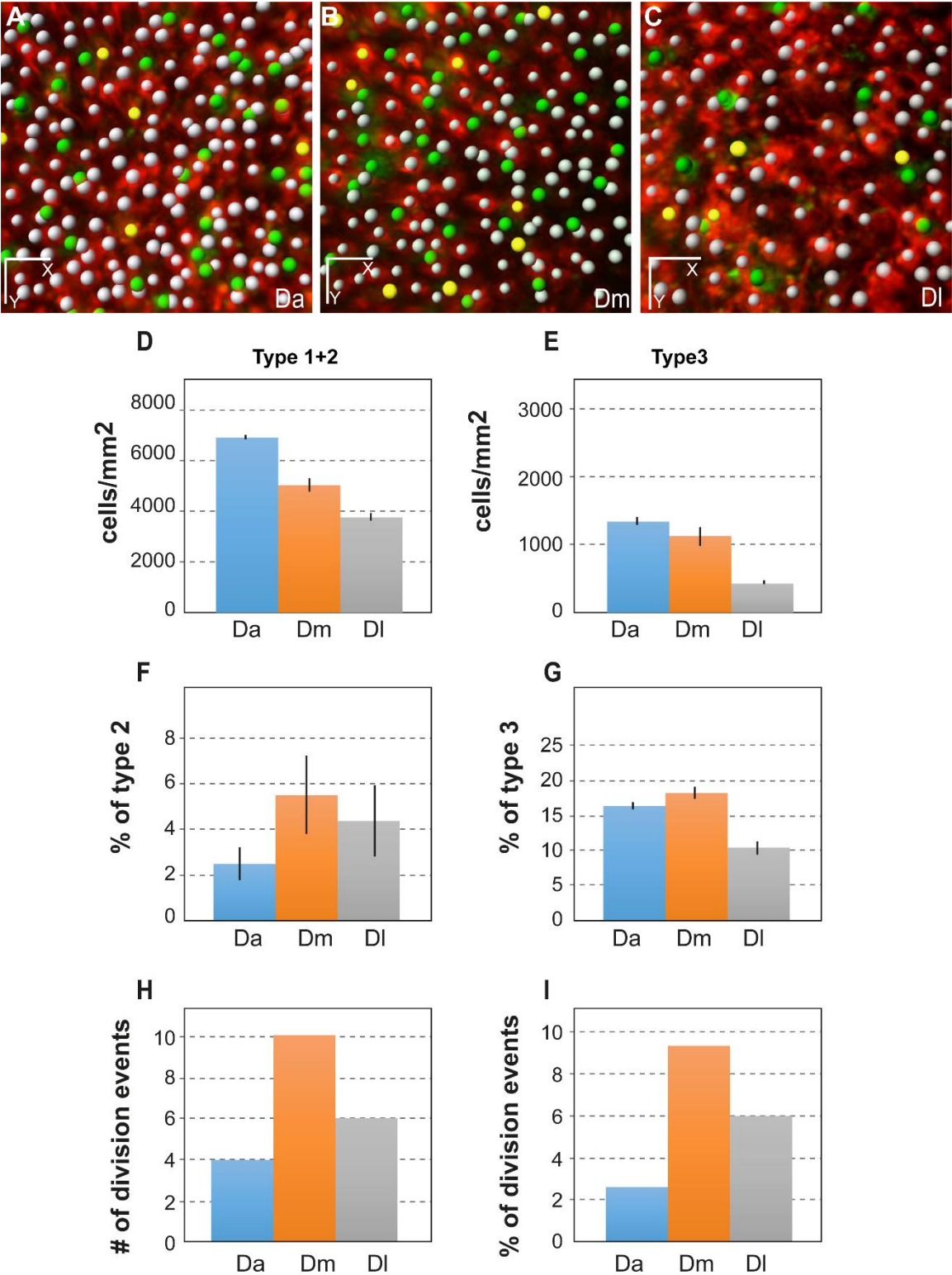
Scale bars: 30 μ m (A-C).



Supplementary material Fig. S10. Plotting of adult neural stem cells and proliferating progenitors at time point 0 on a live image.

Dorsal view of one hemisphere of a *her4:dRFP;mcm5:eGFP;casper* transgenic fish (individual fish named piwi) imaged at t0. (A) red channel only (RG cells) with corresponding plots (white dots), (B) green channel only (proliferating cells), (C) merged red and green fluorescence view with corresponding plots for RG (white) and proliferating progenitors (green), (D) plots only (as in Fig. 2E).

Scale bars: 80 μm (A-D).



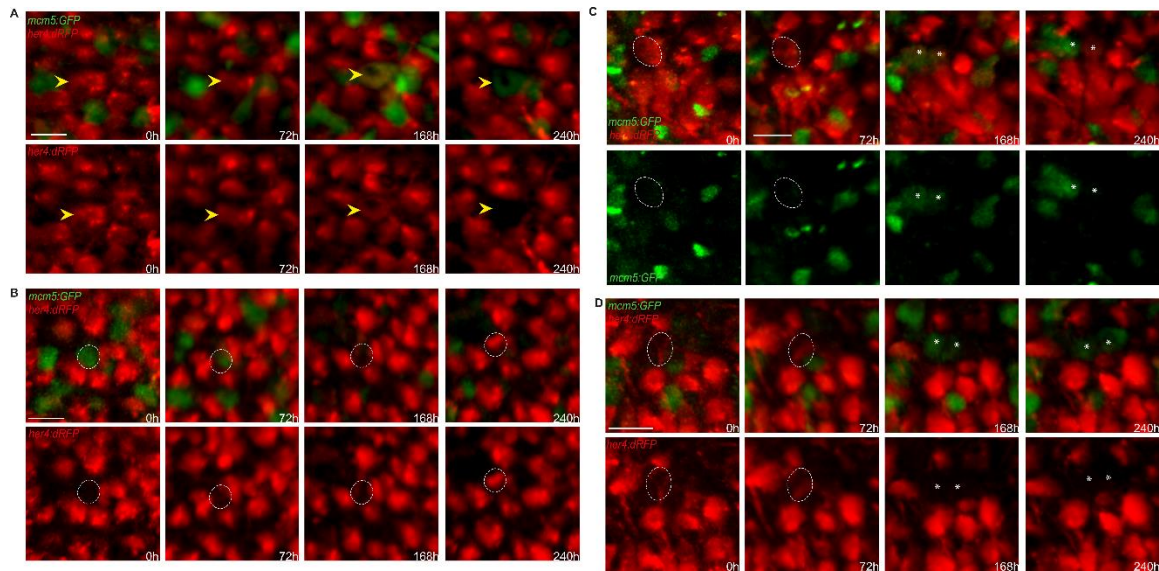
Supplementary material Fig. S11. Quantitative analysis of dynamic NSC parameters in the pallial areas Da, Dm and Dl in the fish named piri.

(A-C) Live images of the pallial germinal zone showing *her4:drfp*-positive NSCs (red) and *mcm5:egfp* dividing cells (green) and in piri, high magnification views of the three domains Da, Dm and Dl, as indicated, with individual cell plotting. White dots: quiescent NSCs (type 1), yellow dots: activated NSCs (type 2), green dots: dividing, *her4:drfp*-negative cells (type 3).

(D-G) Quantification of NSC parameters over 10 days (t1-t4). All statistics are paired t-tests, with standard deviations indicated as vertical bars. The mean numbers of NSCs counted for each domain are 158 (Da), 128 (Dm) and 96 (Dl). (D) NSC density in each domain (color-coded), measured as the total number of type 1 + type 2 cells per mm² of germinal zone surface (see Materials and Methods for the calculation of this surface taking into account the germinal zone curvature). Da/Dm: $p < 0.01$; Da/Dl: $p < 0.0001$; Dm/Dl: $p < 0.01$. (E) Density of type 3 cells (non-glial proliferating progenitors), measured as the total number of type 3 cells per mm². Da/Dm: $p < 0.05$; Da/Dl: $p < 0.1$; Dm/Dl: $p < 0.05$. (F) Proportion of activated NSCs (type 2 cells) in each domain among the total NSC population (type 1 + type 2 cells). Da/Dm: $p < 0.05$; Da/Dl: $p < 0.1$; Dm/Dl: $p < 0.05$. (G) Proportion of type 3 cells among the total progenitor population (type 1 + type 2 + type 3 cells). Da/Dm: $p < 0.05$; Da/Dl: $p < 0.01$; Dm/Dl: $p < 0.01$.

(H,I) Quantification of de novo NSC activation events over 7 days (t2-t4) in absolute numbers (H) and in proportion of the number of RG quiescent at time t4 (I). Da/Dm: $p = 0.03$, significant; Da/Dl: $p = 0.2$, NS; Dm/Dl: $p = 0.6$, NS. , Fischer's 2-tailed test.

Scale bars: 30 μ m (A-C).



Supplementary material Fig. S12. Fluctuations of *her4:drfp* expression preceding or following NSC division.

High magnification (dorsal views) of groups of cells in a *her4:drfp;mcm5:eGFP;casper* transgenic fish (individual fish named piwi) filmed live through the skin and skull over 4 time points (t1-t4) spanning 10 days. Top panels: merged channels, bottom panels: red or green channels only. **(A)** Example of a RG about to divide and switching off *her4:drfp* expression after turning on *mcm5:egfp*. **(B)** Example of a *mcm5:gfp*-positive cell acquiring *her4:drfp* expression, likely after division. **(C)** Additional example of an asymmetric, gliogenic (self-renewing) division. The circle is showing a RG cell expressing RFP only on the first days, switching on *mcm5:egfp* and dividing at t3 and giving rise to two daughter cells (asterisks) one of which expresses RFP only (and harboring a process, not shown) (right cell) and the other maintaining GFP only (left cell). **(D)** Example of a symmetric division where both daughters harbor a non-glial fate at time t4. The circle surrounds the initial RG, and asterisk indicate the position of the two daughters.

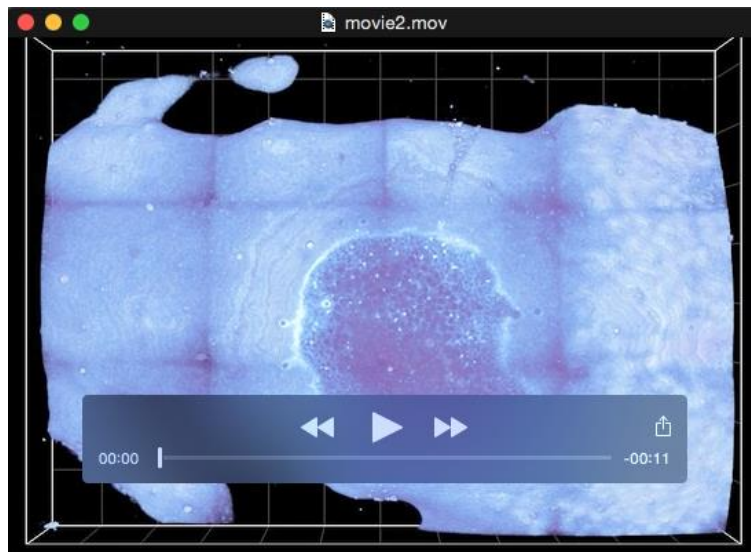
Scale bars: 20 μ m **(A-D)**.

Supplementary Movies



Supplementary Movie 1. Second- and third-harmonic generation (SHG, THG) imaging of the telencephalon region in a live unstained zebrafish adult.

The fish (5 months) was anesthetized and held in an upright microscope. The dataset consists of a mosaic of 12 XYZ stacks, each spanning a volume of $500 \times 500 \times 160 \mu\text{m}^3$, resulting in $2000 \times 1500 \times 160 \mu\text{m}^3$ for the entire image. Excitation wavelength was $\lambda = 1180\text{nm}$. THG signals (at $\lambda/3$) and SHG signals (at $\lambda/2$) were collected through the excitation objective and simultaneously detected on two independent channels. The SHG image, shown in orange, highlights fibrillar collagen and reveals the global structure of the skull. The THG image, shown in blue, highlights interfaces and heterogeneities and provides multiple structural details. In particular, THG signals reveal skin cell boundaries, blood vessels, pigmented cells, skull surface, lipidic accumulations, and myelin fibers. Scale bar, $200 \mu\text{m}$. Voxel size $2 \times 2 \times 2 \mu\text{m}^3$. Time per pixel, $5\mu\text{s}$.



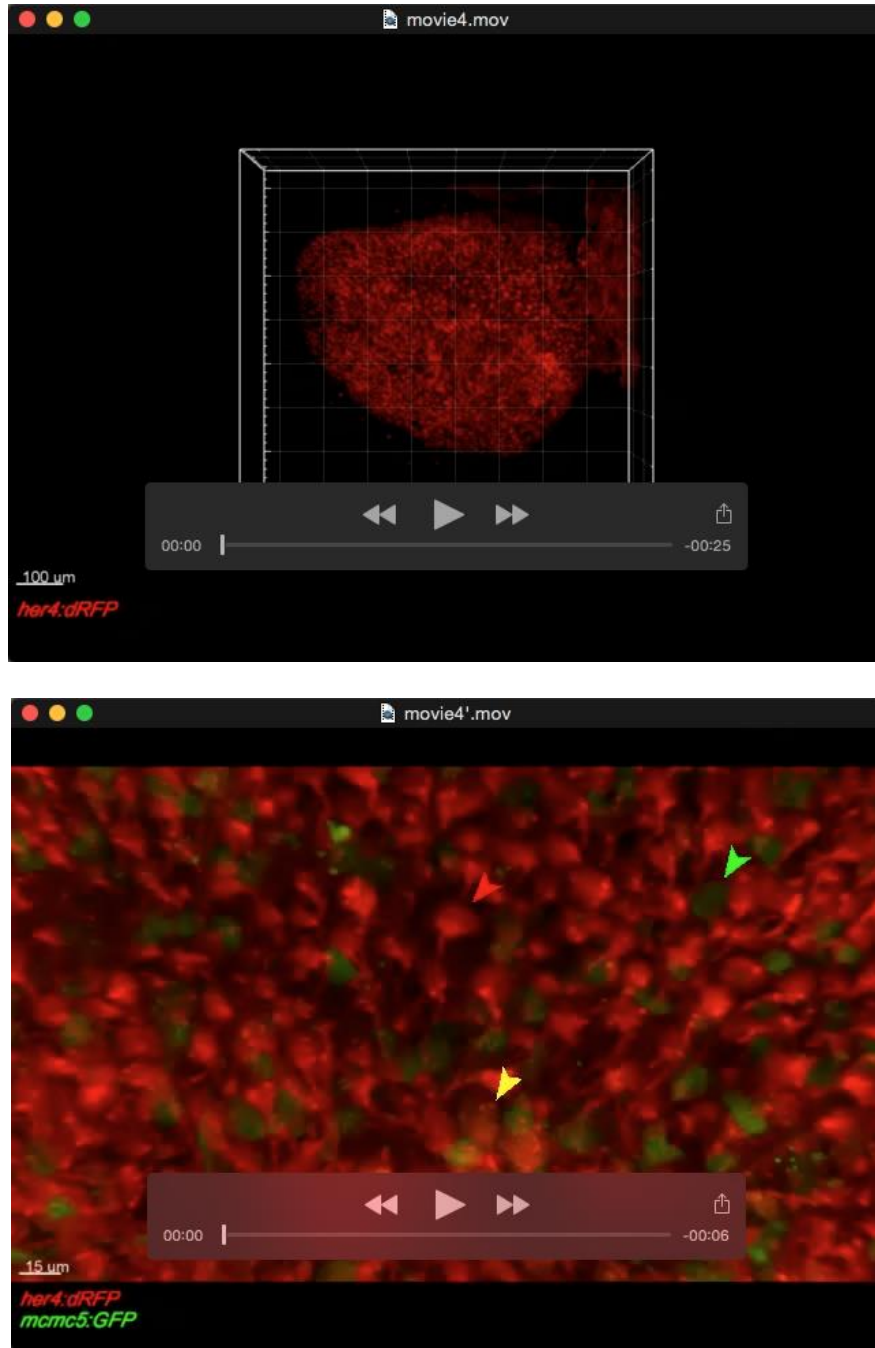
Supplementary Movie 2. THG+SHG imaging of the telencephalon region in a live zebrafish: 3D volume rendering.

3D volume rendering of the dataset shown in Movie1. Grid size is 200 μm .



Supplementary Movie 3. Second-harmonic generation (SHG) imaging of an adult zebrafish skull.

3D rendering of the SHG channel of the dataset shown in Movie1. The skull morphology and suture are clearly visible and provide large-scale landmarks for longitudinal imaging. Grid size is 200 μm .



Supplementary Movies 4 and 4'. 3D animated rendering of the pallial germinal zone from a *her4:dRFP;mcm5:GFP* double transgenic *casper* fish highlighting aNSCs (red) and dividing cells (green).

Individual fish named piwi (as in Figure 2). The beginning of the movie is a diving into the germinal zone at time t1 (red channel only, then red and green channels). At the end, the same germinal zone area is shown at the 4 successive time points (t1-t4). Movie 4' is an extract of the latter time lapse sequence. Red arrow: quiescent RG, yellow arrow: dividing RG; green arrows: dividing progenitors not expressing *her4:drfp*.

Supplementary Table 1. Anesthesia procedure

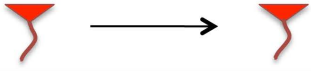
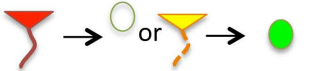
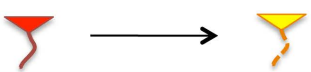
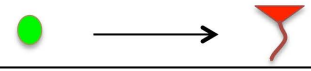
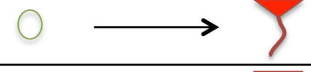
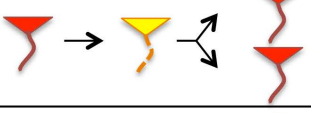
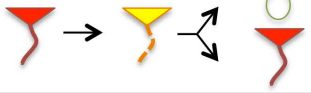

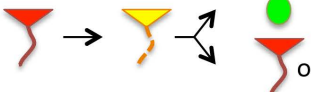



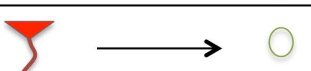
| Test | Induction | Maintenance | Stage | Duration |
|------|--------------------|--|-------|----------|
| 1 | 0.02% MS222 90 sec | Incubation in 0.005% MS222 (50ml changed every 30 min) | 3 | 2 hours |
| 2 | 0.02% MS222 90 sec | Incubation in 0.005% MS222 + 0.005% isoflurane (50ml changed every 30 min) | 4 | 2 hours |
| 3 | 0.02% MS222 90 sec | Intubation with a flow of 0.005% MS222 + 0.005% isoflurane (100 ml/h) | 4 | 2 hours |

Comparison of anesthesia procedures based on Huang et al.²). All procedures use an identical MS222 induction step, but differ in the anesthesia maintenance phase, using (protocols 2 and 3) or not (protocol 1) isoflurane, and relying (protocol 3) or not (protocols 1 and 2) on circulating fluid by intubation. Anesthesia stages are from Keene et al.³), modified from ^{4,5}).

We found that stage 3 (narcosis: partial loss of muscle tone; increased opercular rate; react of equilibrium only to strong tactile and vibrational stimuli) did not lead to sufficient immobilization for long-term imaging, while Stage 4 (light anesthesia: total loss of muscle tone and equilibrium; slow but regular of equilibrium opercular rate; loss of spinal reflexes) was appropriate. We use Protocol 3 for this study.

Supplementary Table 2. NSC fates

Cell counts are based on tracking 1138 cells in the fish named piwi over 4 imaging time points spanning 10 days. *her4:drfp*-positive cells have been considered RG (triangle shape) – although their process could be at times difficult to see or not visible during or immediately after division-. Other progenitors or cells are drawn as ovals. Cells are color-coded as follows: red: dRFP-positive, green: GFP-positive, yellow: both red and green, no colour: no expression of either transgene.

| Cell tracking | Nb | Figure | Possible interpretation |
|--|------|---|--|
| 1  | 1031 | | Quiescence, fate maintenance |
| 2  | 23 | Fig.S12A | Entry into division |
| 3  | 14 | | Entry into division |
| 4  | 16 | Fig.S12B | Re-expression of <i>her4</i> following division |
| 5  | 1 | | Ambiguous Fate change or slow <i>her4</i> fluctuations |
| 6  | 4 | Fig.4C | Gliogenic, symmetric in fate and proliferation status |
| 7  | 12 | Fig.4B (top, magenta) | Gliogenic, asymmetric in fate at t_4 ; fate of  is undertermined |
| 8  | 14 | Fig.4A Fig.4B (bottom, cyan) Fig.S12C | Gliogenic; fate of  is undertermined |
| 9  | 5 | Fig.S12D | Symmetric; fate of  is undertermined |
| 10  | 18 | Fig.4D | Ambiguous Fate change or slow <i>her4</i> fluctuations |

References:

1. White, R.M. et al. *Cell Stem Cell* **2**, 183–189 (2008).
2. Huang, W.-C. et al. *Zebrafish* **7**, 297–304 (2010).
3. Keene, Noakes, D.L., Moccia, R.D. & Soto, C.G. *Aquaculture Research* **29**, 89–101 (1998).
4. McFarland, W.N. *Publ Inst Mar Sci* **6**, 22–55 (1959).
5. Jolly, D.W., Mawdesley-Thomas, L.E. & Bucke, D. *Veterinary Record* **91**, 424–426 (1972).